Analog Integr Circ Sig Process (2008) 55:197–204
DOI 10.1007/s10470-007-9044-x

Non-Fourier thermal conduction in nano-scaled electronic structures

Bjorn Vermeersch · Gilbert De Mey

Received: 18 September 2006 / Accepted: 7 February 2007 / Published online: 25 April 2007
© Springer Science+Business Media, LLC 2007

Abstract When very fast phenomena and small structure dimensions are involved, the classical law of Fourier becomes inaccurate. A more sophisticated model is then needed to describe the thermal conduction mechanisms in a physically acceptable way. In this paper the according diffusion equation is solved for a nano-scaled semiconductor substrate, in order to gain physical insight in the problem. Analytical solutions for the temperature and heat flux distributions are presented. The complex thermal impedance and thermal step response of the structure are discussed. The most remarkable fact is that the temperature inside the substrate can go below the ambient temperature for a short amount of time. The results also clearly demonstrate the wave character of the heat propagation and the analogy with RLC transmission lines.

Keywords Non-Fourier conduction · Nano-scale heat transfer · Thermal waves · Thermal impedance · Hyperbolic diffusion equation

This work concerns a slightly extended version of a paper that was presented at the latest MIXDES Conference (Gdynia, Poland). It is submitted for the Special Issue MIXDES 2006 of the *Analog Integrated Circuits and Signal Processing* journal upon invitation of the MIXDES Scientific Committee.

B. Vermeersch (✉) · G. D. Mey
Department of Electronics and Information Systems, Ghent University, Sint Pietersnieuwstraat 41, Gent 9000, Belgium
e-mail: bjorn.vermeersch@elis.ugent.be

G. D. Mey
e-mail: demey@elis.ugent.be

1 Introduction

In heat transfer applications, thermal conduction is generally modelled by the very well known law of Fourier:

$$\vec{q} = -k\vec{\nabla}T \tag{1}$$

In words: a temperature gradient $\vec{\nabla}T$ [K/m] gives rise to a heat flux $\vec{q}[\mathrm{W/m^2}]$ or vice versa. Both quantities are related through the thermal conductivity k[W/mK], a material dependent parameter.

The main objection to (1) is (the lack of) its behaviour with respect to time. When some sort of heat source is suddenly switched on, one will notice a small but *immediate* temperature rise even for regions at relatively large distances from the source. Since conduction is essentially a mechanical process—heat spreads through the material due to the atoms passing vibrational energy from one to another—this observation is physically not acceptable. In opposition to (1) which allows heat to travel infinitely fast, the velocity of heat propagation is in reality limited to the speed of sound c[m/s] in the material.

1.1 Non-fourier conduction

To overcome this problem, a modification of Fourier's law was proposed by Cattaneo [1] and Vernotte [2]:

$$\vec{q} + \tau\frac{\partial\vec{q}}{\partial t} = -k\vec{\nabla}T \tag{2}$$

which expresses a gradual growth of the heat flux to the classical value $-k\vec{\nabla}T$, with a time constant τ. Expressing the energy balance for an arbitrary volume of the material and taking (2) into account leads to:

$$k\nabla^2 T - C_v \frac{\partial T}{\partial t} - \tau C_v \frac{\partial^2 T}{\partial t^2} = -p - \tau \frac{\partial p}{\partial t} \quad (3)$$

where C_v [J/m^{3}K] is the specific heat per volume unit and p [W/m^3] the power density. Equation (3) is sometimes denoted as the hyperbolic heat equation [3, 4]; setting $\tau = 0$ produces the classical diffusion equation. The third term—being proportional to the second order time derivative—gives rises to thermal wave effects. This indeed ensures a finite velocity for the heat propagation. Identification with the classical wave equation where c must be used as wave speed yields:

$$\tau = \frac{k}{C_v c^2} \quad (4)$$

Additionally it can be shown that the term $\tau C_v(\partial^2 T/\partial t^2)$ can be associated with a thermal inductance. This element shows a temperature drop if the heat flow changes in time (clearly indicating that it as such cannot exist in practice). An arbitrary small portion of a material under non-Fourier conduction can be represented by the network shown in Fig. 1.

1.2 Aims and purpose

For most solid state materials one has $c \approx 5000$ m/s = 5 nm/ps. In the case of silicon with $k = 160$ W/mK and $C_v = 1.78 \times 10^6$ J/m^{3}K, (4) leads to $\tau \approx 3.5$ ps. The very small magnitude of the time constant indicates that for most practical applications, the effects of non-Fourier conduction are negligible. In electronics however things may be somewhat different. As the miniaturisation and tendency towards higher circuit speeds continue, microelectronics push Fourier's law to its limits. For future device generations it is to be expected that thermal wave effects will more and more come into play, and (3) is needed to describe these phenomena properly.

This paper will be dedicated to a theoretical investigation of non-Fourier conduction in a very small semiconductor substrate. On one hand this may give us a glimpse of the (exotic) behaviour that might be expected from tomorrow's electronics. On the other hand the geometry is quite simple, allowing an analytical approach and providing fundamental physical insight.

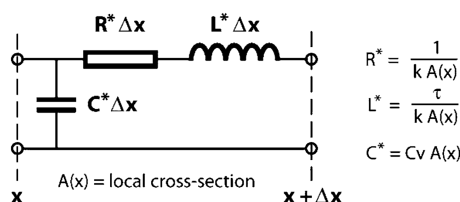

Fig. 1 Section of distributed thermal network representation for non-Fourier conduction (quasi 1-dimensional heat flow assumed)

2 Solution of the heat equation

2.1 Investigated structure

Let us consider a bar-shaped silicon substrate with thickness H and cross-section area A (Fig. 2). The top surface is entirely covered with a uniform heat source dissipating a power density $p_0(t)$ [W/m^2], the bottom plate is perfectly cooled (ambient temperature $T = 0$). The rest of the substrate surface (the side walls) is thermally isolated, i.e., the normal component of the heat flux equals zero. Using (2) this leads to $\partial T/\partial n = 0$, as for the case of classical Fourier conduction.

Due to the geometry of the problem and its boundary conditions, one can see the isothermal surfaces are perpendicular to the side walls. Hence the temperature distribution is one-dimensional, $T = T(x, t)$, and the heat equation can be solved relatively easily.

2.2 Solution in the laplace domain

Since (3) is a partial differential equation it is best solved for the Laplace transform with respect to time $T(x,s) = \mathcal{L}[T(x,t)]$ of the temperature. As there is no power dissipation inside the substrate, i.e., $p = 0$, transformation of Eq. (3) reads:

$$k\frac{\mathrm{d}^2 T(x,s)}{\mathrm{d}x^2} - s(1 + s\tau)C_v T(x,s) = 0 \quad (5)$$

which immediately leads to:

$$T(x,s) = C_1 \cosh(\gamma x) + C_2 \sinh(\gamma x) \quad (6)$$

where

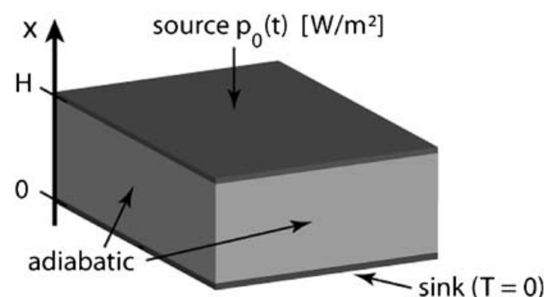

Fig. 2 Silicon substrate completely covered by uniform heat source

$$\gamma = \sqrt{\frac{s(1+s\tau)C_v}{k}} \tag{7}$$

The coefficients C_1 and C_2 are found by applying the boundary conditions at the bottom and top surfaces. For the former we readily have

$$T(0,s) = 0 \tag{8}$$

and for the latter the law of Cattaneo–Vernotte (2) yields:

$$k\frac{\mathrm{d}T(x,s)}{\mathrm{d}x}|_{x=H} = (1+s\tau)p_0(s) \tag{9}$$

The rest of this paper will mainly focus on the thermal step response. In other words, the heat source is suddenly switched on at $t = 0$ and the temperature distribution is studied. Therefore we set:

$$p_0(t) = p_0 \cdot u(t) \Rightarrow p_0(s) = \frac{p_0}{s} \tag{10}$$

in which

$$u(t) = \begin{cases} 0 & t<0 \\ 1 & t>0 \end{cases} \tag{11}$$

is the Heaviside function. Combining (6), (8) and (9) produces:

$$T(x,s) = \frac{p_0(1+s\tau)\sinh(\gamma x)}{ks\gamma\cosh(\gamma H)} \tag{12}$$

From Eq. (12) the heat flux flowing in the $-x$ direction (source to sink) can be derived by applying (2):

$$q(x,s) = \frac{+k}{1+s\tau}\frac{\mathrm{d}T(x,s)}{\mathrm{d}x} = \frac{p_0\cosh(\gamma x)}{s\cosh(\gamma H)} \tag{13}$$

Moreover, if we divide the source temperature $T(H, s)$ by the total power $P(s) = A \cdot p_0(s)$ we obtain the thermal impedance of the substrate:

$$Z_{th}(s) = \frac{H}{kA}\cdot\frac{(1+s\tau)\tanh(\gamma H)}{\gamma H} \tag{14}$$

The thermal impedance is commonly evaluated for $s = j\omega$, providing the thermal frequency response (AC analysis). One can verify that the DC limit $Z_{th}(s \rightarrow 0)$ of (14) produces the correct and well known result for the thermal resistance, i.e., $R_{th} = H/kA$. As Z_{th} does not depend on the particular waveform of the power dissipation, it captures the entire dynamic behaviour of the substrate. Therefore the complex thermal impedance (and more precise its Nyquist plot in particular) can be used for thermal characterization of electronic packages [5–8].

To facilitate the interpretation of the results, we will henceforth work with dimensionless forms of the expressions (12), (13) and (14). The temperature, heat flux and impedance are normalized respectively to the steady state temperature of the source $T_{ss} = T(H, t \rightarrow \infty) = p_0 H/k$, the flux at the source p_0 and the DC impedance R_{th}. Normalized Laplace expressions and their time domain counterparts will be indicated with a tilde. Summarizing:

$$\tilde{T} = \frac{k}{p_0 H}\cdot T, \quad \tilde{q} = \frac{q}{p_0}, \quad \tilde{Z}_{th} = \frac{kA}{H}\cdot Z_{th} \tag{15}$$

2.3 Thermal step response

2.3.1 *Temperature*

The transient behaviour of the temperature in the substrate can be obtained by taking the inverse Laplace transform of $\tilde{T}(x,s)$, being the normalized form of (12). First we write:

$$\begin{aligned}\frac{\sinh(\gamma x)}{\cosh(\gamma H)} &= \frac{e^{-\gamma H}[e^{\gamma x} - e^{-\gamma x}]}{1+e^{-2\gamma H}} \\ &= [e^{\gamma x} - e^{-\gamma x}]\left(e^{-\gamma H} - e^{-3\gamma H} + e^{-5\gamma H} - \ldots\right) \\ &= e^{-\gamma(H-x)} - e^{-\gamma(H+x)} - e^{-\gamma(3H-x)} \\ &\quad + e^{-\gamma(3H+x)} + e^{-\gamma(5H-x)} - e^{-\gamma(5H-x)} - \ldots\end{aligned} \tag{16}$$

This shows that $\tilde{T}(x,s)$ can be written as the summation of terms of the following form

$$\frac{1+s\tau}{s}\cdot\frac{e^{-\gamma a}}{\gamma H} = \frac{1+s\tau}{s}\cdot\phi(s,a) \tag{17}$$

where a takes the form $(2n + 1)H \pm x$. After some manipulation we obtain:

$$\phi(s,a) = \frac{c}{H}\frac{\exp\left(-\frac{a}{c}\sqrt{s(s+1/\tau)}\right)}{\sqrt{s(s+1/\tau)}} \tag{18}$$

for which the inverse Laplace transform is found to be [9]

$$\phi(t,a) = \frac{c}{H}\exp\left(-\frac{t}{2\tau}\right)I_0\left(\frac{1}{2\tau}\sqrt{t^2 - \frac{a^2}{c^2}}\right)u\left(t - \frac{a}{c}\right) \tag{19}$$

with I_0 the modified Bessel function from the first kind with order 0. The remaining factor $\frac{1+s\tau}{s} = \frac{1}{s} + \tau$ in (17) produces the integral and a fraction τ of the function $\phi(t, a)$. The normalized step response temperature is finally given by:

$$\tilde{T}(x,t) = \sum_{n=0}^{\infty}\alpha_n\left(\tau\phi(t,a_n) + \int_0^t \phi(t,a_n)\mathrm{d}t\right) \tag{20}$$

with

$$\alpha_{2i} = (-1)^i, \quad \alpha_{2i+1} = (-1)^{i+1} \tag{21}$$

and

$$a_{2i} = (2i+1)H - x, \quad a_{2i+1} = (2i+1)H + x \tag{22}$$

It is important to point out the presence of $u(t - \frac{a}{c})$ in both $\phi(t, a)$ and $\int \phi(t, a)$. This Heaviside function introduces a time delay $\frac{a}{c}$. A first consequence is that (20) is eventually not an infinite series; starting from $n = 0$, more terms must be gradually included as time progresses. Even more important, these time delays have a physical meaning: $\frac{a}{c}$ is indeed nothing else than the time needed for a wave with speed c to travel a distance a. Moreover, the values (22) for a_n correspond exactly to the total distance traversed at location x by a wave reflecting back and forth between the top and bottom surface of the substrate (Fig. 3). These observations clearly indicate that the hyperbolic diffusion equation gives rise to thermal waves, running at the speed of sound c. These waves are however strongly damped and are only important for very thin substrates, as we will see in a further section. For thicker substrates the wave effects are hardly noticable and they can be neglected. In such cases, as expected, the classical Fourier conduction can be used.

2.3.2 *Heat flux from source towards sink*

Using the method similar to what has been been done for the temperature, $\tilde{q}(x, s)$is found to be composed of terms of the following form:

$$\frac{\exp\left(-\frac{a}{c}\sqrt{s(s+1/\tau)}\right)}{s} \tag{23}$$

Using [9] yields after some manipulation:

$$\tilde{q}(x,t) = \sum_{n=0}^{\infty} \beta_n \int_0^t \psi(t, a_n) \mathrm{d}t \tag{24}$$

where a_n is given by (22),

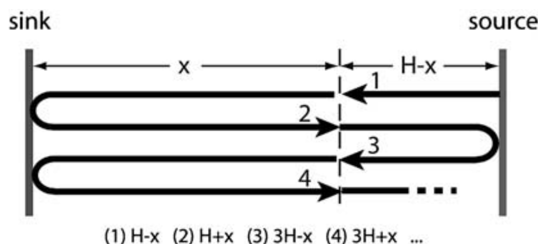

Fig. 3 Physical interpretation of a_n values as total wave travel distance

$$\beta_{2i} = (-1)^i, \quad \beta_{2i+1} = (-1)^i \tag{25}$$

and

$$\psi(t,a) = \exp\left(-\frac{t}{2\tau}\right) \times \left[\frac{a/c\tau}{2\sqrt{t^2 - \frac{a^2}{c^2}}} I_1\left(\frac{1}{2\tau}\sqrt{t^2 - \frac{a^2}{c^2}}\right) u\left(t - \frac{a}{c}\right). + I_0\left(\frac{1}{2\tau}\sqrt{t^2 - \frac{a^2}{c^2}}\right)\delta\left(t - \frac{a}{c}\right)\right] \tag{26}$$

with I_1 the modified Bessel function from the first kind with order 1 and δ the Dirac function. Since $I_0(x \to 0) = 1$, the integration in (24) of the second term of (26) can be simplified and gives rise to

$$\exp\left(-\frac{a}{2c\tau}\right) u\left(t - \frac{a}{c}\right) \tag{27}$$

Like before, the Heaviside functions cause a time delay a_n/c for the n-th term of the heat flux (24). This underlines again the wave character of the solution. The heat travels at a finite speed c through the substrate, consistent with the mechanical nature of the heat propagation stated before. As the a_n values did not change, the physical explanation of Fig. 3 still remains valid.

3 Results and discussion

Further analysis will now be carried out for a silicon substrate with square shaped cross-section (A = 100 nm × 100 nm). The graphs that are presented were produced by plotting Eqs. (14), (20) and (24) with a symbolic mathematics computer program.

3.1 Thermal Impedance

We will study the thermal impedance along the imaginary axis $s = j\omega$, revealing the AC behaviour of the substrate. This information can be interpreted directly in terms of an equivalent electrical distributed network. The most convenient way of representing Z_{th} is using its Nyquist curve, being a plot of $\mathrm{Im}[Z_{th}(j\omega)]$ versus $\mathrm{Re}[Z_{th}(j\omega)]$ with ω as a parameter. Nyquist impedance plots for various substrate thickness values are shown in Figs. 4–7.

For the ‘thick’ 100 nm substrate the results for non-Fourier and classical ($\tau = 0$) conduction are compared (Fig. 4). Whereas the low frequency part of the two curves almost coincide, the high frequency behaviour is quite different. The non-Fourier impedance tends to converge to a value which is not equal to zero. This high frequency (HF) limit can be calculated by taking the limit $s \to \infty$ of (14). After normalization we obtain:

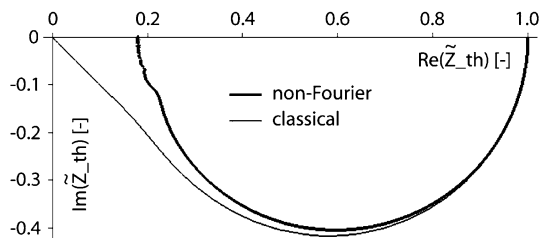

Fig. 4 Nyquist plot of normalized thermal impedance (H = 100 nm)

$$\tilde{Z}_{th,HF} = \frac{kA}{H} \lim_{s\to\infty} Z_{th}(s) = \frac{k}{HcC_v} \tag{28}$$

For H = 100 nm and with the silicon parameters mentioned earlier we get 0.18 which is indeed the value observed on the graph. The result (28) can also be explained physically. Due to the geometry of the substrate, the elements shown in Fig. 1 are all identical (R^*, L^* and C^* are constant). For very high frequencies, such that $\omega L^* \gg R^*$, the series resistance can be neglected. At that point the equivalent distributed network for the substrate is nothing else than a LC transmission line, for which the characteristic impedance is known as

$$Z_0 = \sqrt{\frac{L^*}{C^*}} = \sqrt{\frac{\tau}{kA} \cdot \frac{1}{C_v A}} = \frac{1}{AcC_v} \tag{29}$$

where (4) has been used. Division by R_{th} for normalization gives $\tilde{Z}_0 = \frac{k}{HcC_v}$, being exactly the same result that has been found in (28).

For thinner substrates, some more interesting things start to happen. For H = 50 nm one can notice oscillations of the higher frequency part (Fig. 5). Not surprisingly, the impedance fluctuates around the characteristic impedance of the equivalent transmission line (Eq. (28) now produces 0.36). The most remarkable fact is the Nyquist plot traversing the first quadrant of the complex plane, where $\mathrm{Im}[Z_{th}] > 0$. Such inductive behaviour is not possible for classical Fourier conduction.

As the thickness of the substrate further decreases, the inductive character can even be observed for low frequencies (Figs. 6 and 7). At the same time the high

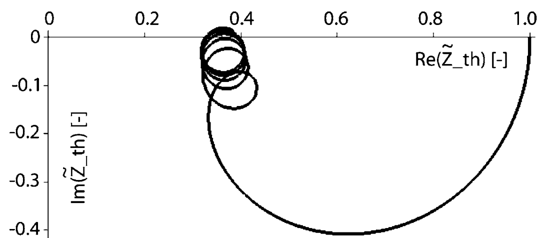

Fig. 5 Nyquist plot of normalized thermal impedance (H = 50 nm)

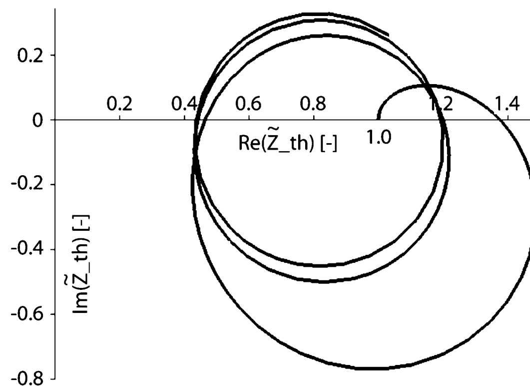

Fig. 6 Nyquist plot of normalized thermal impedance (H = 25 nm)

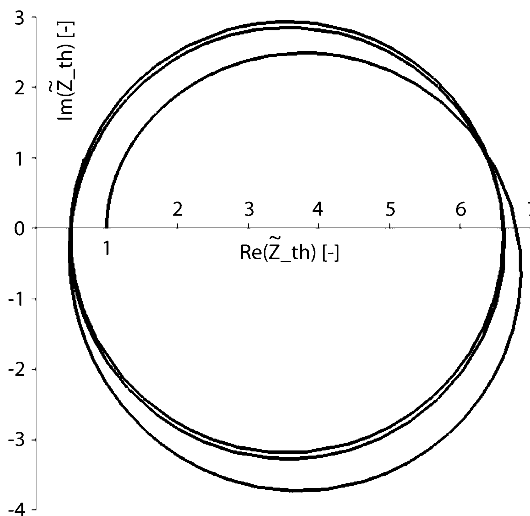

Fig. 7 Nyquist plot of normalized thermal impedance (H = 10 nm)

frequency fluctuations start to grow dramatically. As the frequency is increased the impedance curve tends to a circle, with its origin located on the real axis. This fact can be proven by a profound analysis of (14). As can be seen on the Nyquist plots, the circle becomes bigger and is moved to the right as the substrate gets thinner.

One remarkable observation for the 10 nm case is that the radius of the normalized impedance circle is relatively large compared to 1. Hence the magnitude of the impedance is significantly exceeding the steady-state value in certain frequency ranges. This is important from a reliability point of view, since the temperature of a device operating in this frequency range will be wildly oscillating between very high and sub-ambient values.

3.2 Transient step response

Throughout the graphs, the time scale has been normalized to a value H/c. This is the time a wave needs to travel between the heat source and the bottom of the substrate.

The results presented here have been carefully checked. Comparison to those obtained by numerical inverse Fourier transform of (12) and (13) showed a very good agreement. The numerical method is much faster, but as it produces a lot of numerical noise (rapid fluctuations around the analytical plot) these results will not be shown here.

We will mainly focus on a very thin substrate: $H = 10$ nm. Note that for this case the 'wave time' H/c is only 2 ps. Temperature and heat flux for different locations in the substrate after source switch-on at $\tilde{t} = 0$ are shown in Fig. 8.

To begin with, the horizontal lines for the normalized bottom temperature and heat flux at the top (values 0 and 1 respectively) should be noted. They prove that the solutions (20) and (24) fulfill the boundary conditions.

Second, the wave character can be observed very clearly. Both temperature and heat flux show discontinuities. Due to the normalization choice of the time scale, the moment at which these steps occur at various depths can be easily understood by tracking the position of the wavefront as shown in Fig. 3.

Third, we focus on the non-zero starting value for the source temperature. Immediately after it is switched on (thus corresponding to very high frequencies) the source 'feels' a LC transmission line, hence:

$$T(H, 0+) = Ap_0 \cdot Z_0 \overset{(29)}{\Rightarrow} \tilde{T}(H, 0+) = \frac{k}{HcC_v} \qquad (30)$$

giving 1.80 as observed in Fig. 8(a). From (12) it can be demonstrated that for all other locations $0 \leq x < H$ the starting value for the temperature identically equals 0, in accordance with the time delays involved. As time progresses, one can see the temperature and flux are converging towards their (classical) steady state values, namely x/H and 1 respectively.

Finally and most remarkable, a rather exotic behaviour is noticed. Although the heat source is continuously injecting energy into the substrate, temperatures can decrease for a while. During some periods of time, circled in Fig. 8, even negative temperatures (or in better words, below ambient) are observed. It should be stressed that this is *not* a violation of the second nor third law of thermodynamics. Considering the second, it tells in which direction a process should evolve spontaneously, e.g. heat flows from higher to lower temperatures. In this point of view, temperature decrease while heating seems impossible. However, such happens only during a very short time. Also, thermodynamic laws try to describe equilibrium, whereas non-Fourier conduction especially aims at a correct description of the transient behaviour. About the third law, suppose (as a 'Gedankenexperiment') the substrate is placed in an environment at absolute zero. According to

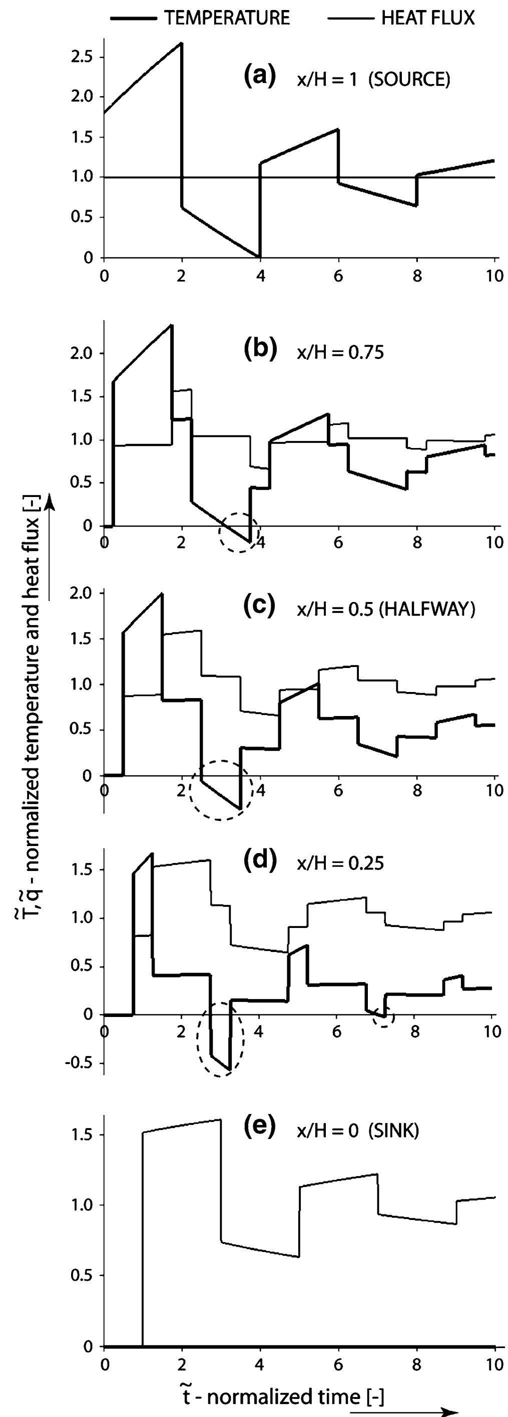

Fig. 8 Temperature and heat flux at various depths in the substrate as function of time (H = 10 nm)

Debye, for very low temperatures we have $C_v \propto T^3$ [10]. The problem now becomes non-linear and the solution derived earlier for the heat equation is no longer valid.

In addition, the negative temperatures may be caused by the rather strict boundary condition $T(0, t) = 0$. As the initial temperature wave approaches the bottom, a virtual

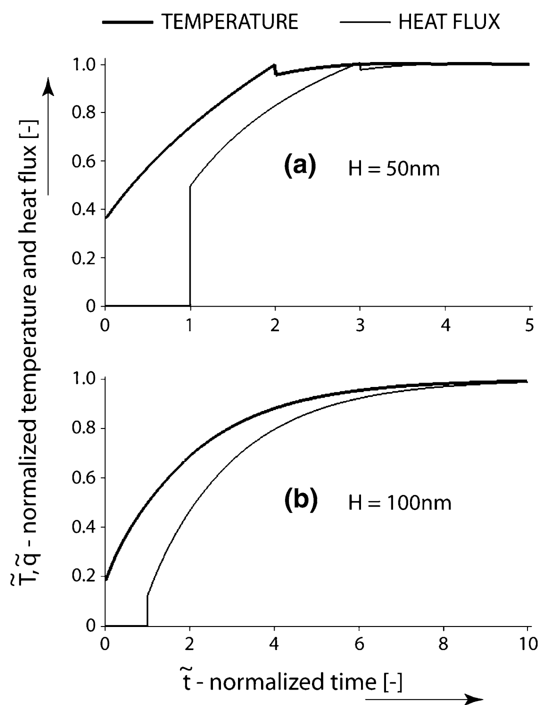

Fig. 9 Source temperature and heat flux at the bottom for various substrate thicknesses

negative wave coming from the opposite direction (leading to the reflection of the incident wave) is induced to force the temperature at zero value. Considering the substrate on top of a much larger carrier material with large heat capacity (e.g. copper), such that the interface is nearly isothermal, might be more realistic. This will be the subject of future work. The suggested extension might also pave the way for experimental verifications, since the situation currently presented is nearly impossible to achieve in practice. Establishing a uniform heat dissipation on top of a very thin layer while keeping the bottom perfectly cooled would be extremely difficult. Also the temperature measurement is posing problems, as the non-Fourier phenomena are occuring at time scales of no more than a few picoseconds. Further research including a second, much thicker, material on which a thin layer is deposited may help to overcome these practical considerations. It should be noted that the analysis which is presented here is only meant as a first step to gain more insight into non-Fourier thermal conduction, and to illustrate that thermal wave-like behaviour is observed when considering very small structures.

For thicker substrates, the discontinuous behaviour including the negative temperatures disappears gradually. The normalized source temperature and bottom heat flux for $H = 50$ and 100 nm are presented in Fig. 9.

The results start looking quite similar to the classical conduction solutions, however two obvious differences are noticed. The non-Fourier conduction manifests itself in the presence of a time delay, due to the finite heat propagation speed, and the non-zero initial source temperature.

4 Summary and conclusions

The Cattaneo-Vernotte model has the potential of growing indespensible in microelectronics design: due to high circuit speed and extremely small dimensions of the devices, the finite velocity of heat propagation can no longer be neglected. Non-Fourier conduction in a semiconductor substrate has been studied by means of analytical solutions for the temperature, heat flux and thermal impedance. The thermal behaviour for very fast phenomena (high frequencies) has been successfully explained by a transmission line equivalence. Especially for very thin substrates, thermal waves are clearly noticed. The wave character gives rise to effects which do not occur under classical Fourier conduction. Key observations are inductive behaviour, discontinuities in the thermal step response, and negative (subambient) temperatures while heating. The latter may be induced by the perfect heat sink boundary condition; more attention will be dedicated to this problem in further research.

Acknowledgments B. Vermeersch is preparing a PhD as a Research Assistant for the Research Foundation—Flanders (FWO—Vlaanderen) and wishes to thank FWO for supporting the presented work.

References

1. Cattaneo, C. (1958). Sur une forme de l'equation de la chaleur eliminant le paradoxe d'une propagation instantanee (in French). *Comptes rendus de l'Académie des sciences, 247*, 431–433.
2. Vernotte, P. (1958). Les paradoxes de la theorie continue de l'equation de la chaleur (in Frenh). *Comptes rendus de l'Académie des sciences, 246*, 3154–3155.
3. Codecasa, L. (2005). Thermal networks from heat wave equation. *IEEE Transactions on Components and Packaging Technologies, 28*, 14–22.
4. Haji-Sheikh, A., Minkowycz, W. J., & Sparrow, E. M. (2002). Certain anomalies in the analysis of hyperbolic heat equation. *Transactions of the ASME—Journal of Heat Transfer, 124*, 307–319.
5. Kawka, P. (2005). Thermal impedance measurements and dynamic modelling of electronic packages (PhD thesis). Ghent University (Gent, Belgium).
6. De Mey, G., Vermeersch, B., & Kawka, P. (2005) Thermal impedance simulations of electronic packages. *In Proceedings of the 12th Internation Conference on Mixed Design of Integrated Circuits and Systems (MIXDES 2005)*, Krakow, Poland, pp. 267–269.
7. Vermeersch, B., & De Mey, G. (2006). Thermal impedance plots of micro-scaled devices. *Microelectronics Reliability, 46*, 174–177.

8. Kawka, P., De Mey, G., & Vermeersch, B. Thermal characterization of electronic packages using the Nyquist plot of the thermal impedance. Accepted with required revisions for publication in IEEE Transactions on Components and Packaging Technologies (under review).
9. Abramowitz, M., & Stegun, I. A. (Eds.) (1970). *Handbook of mathematical functions*. New York, USA: Dover Publications.
10. Debye, P. (1912). *Ann. d Physik, 39*, 789.